International Scientific Conference 20 UNITECH 26

INTERNATIONAL SCIENTIFIC CONFERENCE
19-21 November 2026
GABROVO

MOLECULAR DYNAMICS STUDY OF THE SIZE-DEPENDENT MELTING BEHAVIOR OF CERIUM NANOPARTICLES

Cem Canan[1], Unal Domekeli [2], Murat Celtek [3]

[1]Edirne Vocational College of Technical Science, Trakya University, 22030, Edirne – Türkiye
[2]Dept. of Physics, Trakya University, 22030, Edirne – Türkiye
[3]Faculty of Education, Trakya University, 22030, Edirne – Türkiye

……

**Corresponding author: cemcanan@trakya.edu.tr*

Abstract

Cerium (Ce) is a significant rare-earth element that plays a role in both scientific research and technological applications, owing to its unique phase transitions and distinct physical and structural properties. Investigating the dynamic and structural characteristics of nanoparticles, which vary according to size, is crucial for understanding material behavior at the atomic level. The aim of this study is to determine the melting temperatures of spherical Ce nanoparticles and to investigate their structural changes at the atomic level. The embedded atom method (EAM) was employed to describe interatomic interactions, and Ce nanoparticles of five different diameters were modeled using molecular dynamics simulations. To examine the effects of particle size on the melting process, the systems' potential energies, pair distribution functions, and mean square displacements were calculated. The results indicate that the melting temperature of Ce nanoparticles increases with particle size, and that structural and dynamic properties depend on both temperature and particle size.

Keywords: Cerium, Nanoparticle, Melting, Molecular Dynamics, Embedded Atom Method

INTRODUCTION

Ce is a rare earth element that belongs to the lanthanide group and has an important role in many industrial and technological applications due to its unique chemical properties [1]. It is found in nature mostly in minerals such as monatize and bastnassite, it has the ability to transition between Ce^{3+} and Ce^{4+} oxidation states. This behavior forms the basis of Ce's ability to store and release oxygen, making it useful in lots of chemical processes [2], [3]. Ce and its compounds are used in a wide range of areas such as catalysts, fuel additives, glass and ceramic production, polishing materials and medical applications [4], [5], [6]. This wide range of applications of Ce in technology also makes it important to understand its crystal structure and electronic properties. Studies in the literature have observed that during the transition of Ce from the γ phase to the α phase, it shows a significant volume contraction and it has been noted that this transformation is related to 4f electrons [7]. The physical and structural properties of materials, along with their chemical compositions and crystal structures, also depend on their sizes. As the nanoparticle size decreases, the melting temperature decreases; this change also affects the chemical activity of the material [8], [9]. Valkealahti and Manninenand [10] and Garcia-Rodeja et al. [11] showed in their molecular dynamics (MD) studies on metal clusters that the melting temperature changes depend on cluster sizes, decreasing as the size gets smaller. In this study, we investigated the melting mechanism of Ce nanoparticles (NPs) with different sizes during the heating process using MD simulations with an EAM [12] force field.

This is an open access article licensed under Creative Commons Attribution 4.0 International
Print ISSN: 1313-230X, Online ISSN: 3033-1404

EXPOSITION

In this study, we used the EAM which is a semi-empirical interatomic potential that considers the electron density and embedding energy around the atom to help us understand the many-body interactions between Ce atoms. The total energy of a system consisting of *N* atoms is expressed as [13];

$$E_T = \sum_{i=1}^{N} \left[\frac{1}{2} \sum_{i \neq j}^{N} \emptyset(r_{ij}) + F_i(\rho_i) \right]. \quad (1)$$

Here, $\emptyset(r_{ij})$ represents the pairwise interaction between atoms *i* and *j*. $F_i(\rho_i)$ is the embedding energy dependent on the local electron density at atom *i*. ρ_i consists of the sum of the electron density contributions from the neighboring atoms surrounding atom *i*. r_{ij} denotes the distance between atoms *i* and *j*. EAM potentials data taken from Sheng [14] were used to characterize the interactions between the Ce atoms. We used LAMMPS (Large-scale Atomic/Molecular Massively Parallel Simulator) [15] programmer, for all MD simulations of the bulk and nanoparticles systems which is enables parallel computing. We used NPs of five different sizes to analyze the size effect during melting process. NPs diameters and the number of atoms are shown in Table 1.

Table 1. *The diameter (d) and number of atoms (N) of Ce NPs.*

Symbol	d(nm)	Number of atoms (N)
NP-1	5.0	1908
NP-2	7.0	5204
NP-3	9.0	11116
NP-4	12.0	26336
NP-5	15.0	51371

The Ce NPs were created from the ideal face-centered-cubic (fcc) crystal structure. Firstly, fcc crystal structure was created according to the lattice parameter *(a_0= 5.161 Å)* determined for Ce then spherical NPs were achieved by selecting the atoms within a radius corresponding to the center of NP. The bulk Ce system was simulated in the constant pressure-temperature NPT ensemble under periodic boundary conditions, while the NPs were modeled in the constant volume-temperature NVT ensemble within simulation cell with non-periodic boundary conditions were applied and a vacuum area was created around the NPs. Newton's second law of motion was numerically integrated using the velocity-Verlet algorithm and the time step was set to 1 fs. The temperature and pressure of the system controlled by the Nose-Hoover [16] thermostat and borastat. To obtain the stable structure at 0 K, the system was first annealed for 100,000 steps at a temperature of 300 K, and then cooled to 0 K at a rate of 0.01 K/ps. This process was carried out to reduce the energy of the NPs, which was initially formed from the ideal fcc structure, and to allow the surface atoms to relax into more stable positions then we accepted the structure obtained from this process as the stable initial configuration to examine temperature-dependent properties. The temperature was then increased in 50 K steps starting from 0 K. Around the melting point, the temperature was reduced to 20 K to perform a more detailed temperature scan. At each temperature the simulation was run for 100 ps to reach the equilibrium. Once the system reached equilibrium, the data was collected to calculate time averaged features over 50 ps. After completing the simulation at a given temperature, the resulting atomic configuration was used as the initial structure for the next temperature level. This process was repeated until the temperature range within which the system's melting behavior was observed.

In metals, melting occurs as a first-order phase transition, during which the system's energy changes suddenly and discontinuously. Therefore, the temperature-dependent variation in potential energy is a useful feature for predicting melting behavior. In this study, Figure 1 shows a comparison of the temperature-dependent changes in potential energy per atom of bulk and Ce NPs.

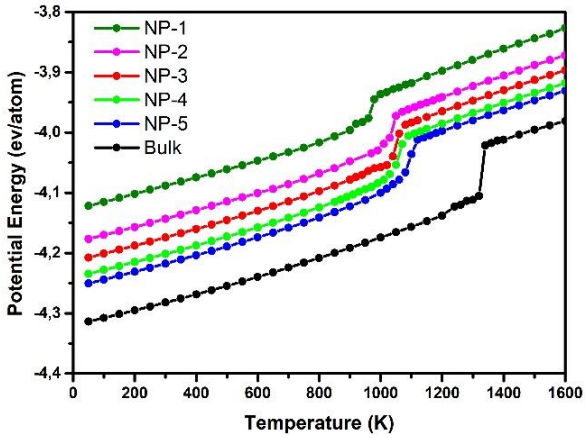


Fig. 1. *Temperature dependence of potential energy for Ce NPs and bulk system*

The MD results presented in Figure 1 clearly show the significant effect of NP size on the thermal stability of the system and phase transition mechanisms. The sudden increases in potential energy observed as a function of temperature represent the solid-liquid phase transition. With decreasing NP size (from NP-5 to NP-1), there is an increase in potential energies and a systematic decrease in melting temperatures. This is because the decreasing particle size reduces the surface-to-volume ratio and therefore increases the number of unstable surface atoms with low coordination number. In particular, it can be seen that for NP-3, NP-4 and NP-5 the changes in potential energy curves are not perfectly sharp and clear, this can be explained by the fact that there is no homogeneous melting within the temperature range but simultaneous coexistence of solid and liquid phases. The structural changes in these regions also examined using snapshots obtained from MD simulations, are given in Figure 2 and it was observed that the melting process progresses gradually, starting from the surface.

The pair distribution function (PDF) *g(r)* is a statistical tool to examine the short-range distribution of atom pairs in a given volume and the general expression is as follows [17]

$$g(r) = \frac{\Omega}{N^2}\langle \sum_i^N \sum_{i \neq j}^N \delta(r - r_{ij}\rangle \qquad (2)$$

where N and Ω represent the number of atoms, and the volume of the simulation cell, respectively.

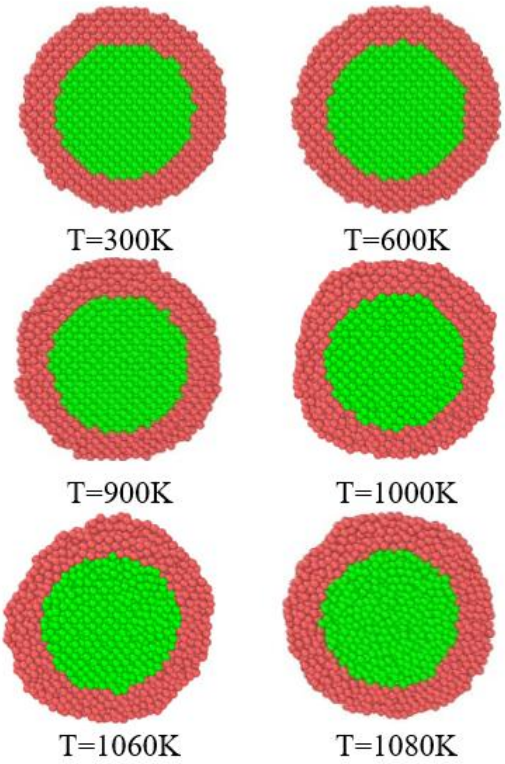


Fig. 2. *Snapshots of the NP-4 during the heating process*

Figure 3 illustrates the PDFs of Ce NP-3 at different temperatures. The clear and sharp peaks in $g(r)$ observed at 300K, also observed in long-range interactions, indicate that the NPs keeps its ordered fcc crystal structure at low temperatures. With the increase in temperature to higher values, it's seen that the peaks expand and the peak heights decrease. Although the long-range crystal order has mostly disappeared at 1040 K, there are still signs that the solid and liquid phases coexist in the structure. At 1060K, the structure becomes fully disordered, and NP completely become liquid. The melting temperatures determined for nanoparticles of different sizes were found to be 960 K, 1030 K, 1050 K, 1080 K, and 1120 K, for NP-1, NP-2, NP-3, NP-4, NP-5 while this value is determined as 1320 K for bulk Ce.

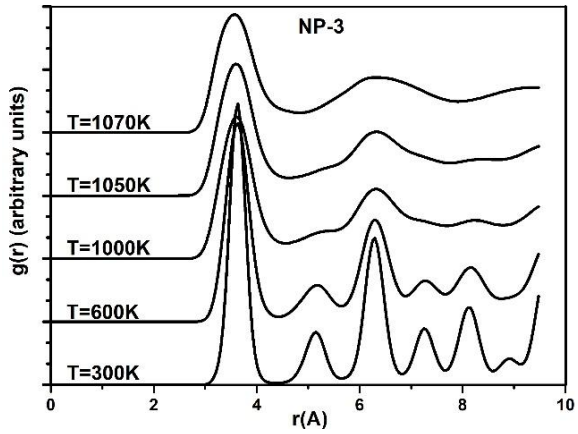


Fig. 3. *PDFs of Ce NP-3 at different temperatures during heating process*

The time-dependent change of the calculated mean square displacement (MSD) values for Ce NP-3 at different temperatures is shown in Figure 4. The most significant result shown in the graph is the visible increase in the slope of the MSD curve as the temperature rises. The MSD value close to zero at 300 K and change very little over time at 1000 K, the slopes of the curves are very low, means that the atoms make small vibrations around their equilibrium positions and the structure keeps its solid character.

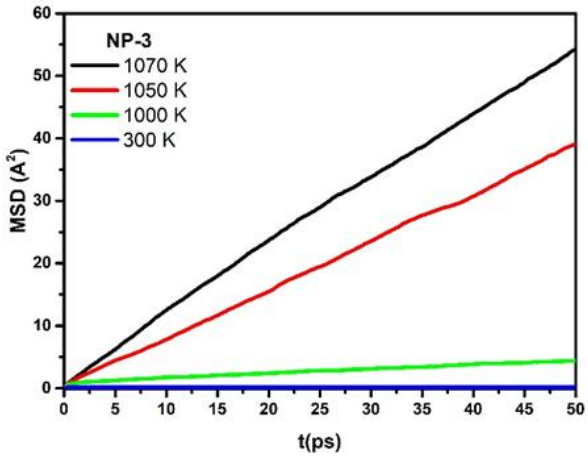


Fig. 4. *Time-evolution changes of MSDs obtained at different temperatures for Ce NP-3.*

MSD analyses reveal the changes in atomic mobility and structural transformation of the NP with increasing temperature during the melting process. The significant increase in MSD values over time at 1050 K indicates that the mobility of the atoms has increased and that the system contains both the ordered structure characteristic of the solid phase and the mobile atoms characteristic of the liquid phase. This suggests that the NP is undergoing a partial melting process and supports the findings obtained from the structural analyses. The significant increase in the slope of the MSD curve observed with increasing temperature to 1070 K indicates that the average displacement of the atoms has accelerated. The substantial increase in atomic mobility at this temperature shows that the structural order characteristic of the solid phase has disappeared and the NP has completely transitioned to the liquid phase. Therefore, the MSD results reveal that atomic mobility gradually increases during the melting process and that complete liquefaction occurs at 1070 K.

CONCLUSION

In this study, we have investigated the melting behavior of Ce nanoparticles using molecular dynamics simulation with EAM potentials. The results obtained in this study have showed that the thermal behavior of Ce nanoparticles is strongly dependent on particle size. It has been observed that the melting temperature increases with increasing nanoparticle size, but the melting temperatures of nanoparticles are lower than the melting temperature of the bulk system. The change in nanoparticle size, along with the melting temperature, also affects the progression of the melting process and atomic mobility. In small nanoparticles, the effects of surface atoms are more pronounced, which reduces the thermal stability of the particles; as the size increases, the effect of the bulk structure becomes more pronounced. When structural and dynamic analyses are evaluated together, the melting of Ce nanoparticles is a continuous process, beginning at the surface of the particle and progressing toward the interior. The conclusions of this study confirm that surface effects play a significant role in understanding the size-dependent thermal and structural behavior of Ce nanoparticles.

ACKNOWLEDGMENTS: *We would like to thank Trakya University Rectorate for giving permission and contributing to present this study as a paper*

REFERENCE

[1] K. N. Delfrey, *Rare earths : research and applications*. Nova Science Publishers, 2008.

[2] S. Atri, B. S. P. Shilpa, and R. Tomar, "Introduction to Cerium and Cerium-based Materials," in *Cerium-Based Materials: Synthesis, Properties and Applications*, Bentham Science Publishers, 2023, pp. 1–13. doi: 10.2174/9789815080087123010003.

[3] N. A. Piro, J. R. Robinson, P. J. Walsh, and E. J. Schelter, "The electrochemical behavior of cerium(III/IV) complexes: Thermodynamics, kinetics and applications in synthesis," *Coord. Chem. Rev.*, vol. 260, pp. 21–36, Feb. 2014, doi: 10.1016/j.ccr.2013.08.034.

[4] Aleksey. Izyumov and Gulnaz. Plaksin, *Cerium : molecular structure, technological applications and health effects*. Nova Science Publisher's, Inc., 2013.

[5] E. Aneggi, C. de Leitenburg, M. Boaro, P. Fornasiero, and A. Trovarelli, "Catalytic applications of cerium dioxide," in *Cerium Oxide (CeO_2): Synthesis, Properties and Applications*, Elsevier, 2020, pp. 45–108. doi: 10.1016/B978-0-12-815661-2.00003-7.

[6] A. Awasthi, Y. Agarwal, and R. Chandra, "Biological, Biomedical and Pharmaceutical Application of Cerium-based Materials," in *Cerium-Based Materials: Synthesis, Properties and Applications*, Bentham Science Publishers, 2023, pp. 92–111. doi: 10.2174/9789815080087123010007.

[7] B. Johansson, W. Luo, S. Li, and R. Ahuja, "Cerium; Crystal structure and position in the periodic table," *Sci. Rep.*, vol. 4, 2014, doi: 10.1038/srep06398.

[8] A. V. Fedorov, A. V. Shulgin, and S. A. Lavruk, "Description of melting of aluminum nanoparticles," *Combust. Explos. Shock Waves*, vol. 52, no. 4, pp. 457–462, Jul. 2016, doi: 10.1134/S0010508216040092.

[9] T. X. T. Sayle, L. W. L. Sayle, and D. C. Sayle, "Liquid crystal seed nucleates liquid–solid phase change in ceria nanoparticles," *Physical Chemistry Chemical Physics*, vol. 17, no. 6, pp. 4441–4447, 2015, doi: 10.1039/C4CP05499G.

[10] S. Valkealahti and M. Manninen, "Structural transitions and melting of copper clusters," *Zeitschrift für Physik D Atoms, Molecules and Clusters*, vol. 26, no. 1, pp. 255–257, Mar. 1993, doi: 10.1007/BF01429161.

[11] J. García-Rodeja, C. Rey, L. J. Gallego, and J. A. Alonso, "Molecular-dynamics study of the structures, binding energies, and melting of clusters of fcc transition and noble metals using the Voter and Chen version of the embedded-atom model," *Phys. Rev. B*, vol. 49, no. 12, pp. 8495–8498, Mar. 1994, doi: 10.1103/PhysRevB.49.8495.

[12] M. S. Daw and M. I. Baskes, "Embedded-atom method: Derivation and application to impurities, surfaces, and other defects in metals," *Phys. Rev. B*, vol. 29, no. 12, pp. 6443–6453, Jun. 1984, doi: 10.1103/PhysRevB.29.6443.

[13] U. Domekeli and M. Celtek, "Structural And Dynamic Properties Of Aluminum Nanoparticles During The Melting Process," UNITECH-2024 *Unitech – Selected Papers*, 2024, doi: 10.70456/FPWL9501.

[14] H. Sheng, EAM potentials, (2026). "https://sites.google.com/site/eampotentials/ce"

[15] S. Plimpton, "Fast Parallel Algorithms for Short-Range Molecular Dynamics," *J. Comput. Phys.*, vol. 117, no. 1, pp. 1–19, Mar. 1995, doi: 10.1006/jcph.1995.1039.

[16] S. Nosé, "A unified formulation of the constant temperature molecular dynamics methods," *J. Chem. Phys.*, vol. 81, no. 1, pp. 511–519, Jul. 1984, doi: 10.1063/1.447334.

[17] U. Domekeli and M. Celtek, "A Molecular Dynamics Simulation Study of the Melting and Solidification Processes of Hafnium Nanoparticles," *Langmuir*, vol. 42, no. 38, pp. 28003–28016, Sep. 2026, doi: 10.1021/acs.langmuir.6c02920.